Journal of Pharmacological and Toxicological Methods 108 (2021) 106956

Contents lists available at ScienceDirect

Journal of Pharmacological and Toxicological Methods

journal homepage: www.elsevier.com/locate/jpharmtox

Genomics Integrated Systems Transgenesis (GENISYST) for gain-of-function disease modelling in Göttingen Minipigs

Joachim Maxeiner [a], Rahul Sharma [a,b], Carolin Amrhein [a], Frederic Gervais [c], Maria Duda [a], Jonathan Ward [a], Lars Friis Mikkelsen [d], Roy Forster [c,*], Michal Malewicz [a,*], Jaya Krishnan [a,b,*]

[a] Genome Biologics, Theodor-Stern-Kai 7, 60590 Frankfurt am Main, Germany
[b] Institute of Cardiovascular Regeneration, Centre for Molecular Medicine, Goethe-University Frankfurt, Theodor-Stern-Kai 7, 60590 Frankfurt am Main, Germany
[c] Citoxlab France, BP563, 27000 Evreux, France
[d] Ellegaard Göttingen Minipigs A/S, Soroe Landevej 302, 4261 Dalmose, Denmark

ARTICLE INFO

Keywords:
Minipig
Transgenics
Gain-of-function
AAV

ABSTRACT

Göttingen Minipigs show several anatomical, physiological, and pathogenetical similarities to humans and serve an important role in translational studies for example as large animal models of disease. In recent years, the number of transgenic Göttingen Minipigs models has increased, as advanced genetic techniques simplify the generation of animals with precisely tailored modifications. These modifications are designed to replicate genetic alterations responsible for human disease. In addition to serving as valuable large animal disease models, transgenic Göttingen Minipigs are also considered promising donors for xenotransplantation. Current technologies for generation of transgenic minipigs demand a long development and production time of typically 2–3 years. To overcome this limitation and expand the use of Göttingen Minipigs for disease modelling and drug testing, we developed the GENISYST (Genomics Integrated Systems Transgenesis) technology platform for rapid and efficient generation of minipigs based transgenic disease models. As proof of concept, we report the successful generation of transgenic minipigs expressing green fluorescent protein (GFP) in multiple disease-relevant tissues including liver, heart, kidney, lungs, and the central nervous system (CNS). Our data demonstrates the feasibility, efficiency, and utility of GENISYST for rapid one-step generation of transgenic minipigs for human disease modelling in drug discovery and development.

1. Introduction

Development of new candidate drugs requires the use of animals during the pre-clinical phase in order to identify substances with highest efficacy and lowest possible toxicity prior to clinical testing in human subjects. Large animals commonly used by the industry include dogs, pigs including minipigs and non-human primates. Pigs in general are model animals that are closest to humans (except for non-human primates) in terms of anatomy, physiology and biochemical metabolism (Forster et al., 2010). In addition, pigs offer the advantage of early sexual maturity, short generation time, high litter number and the possibility of introducing precise genetic modifications (Luo, Lin, Bolund, Jensen, & Sorensen, 2012; Rogers et al., 2008). Pigs are omnivores and their dietary needs and nutritional requirements resemble that of humans, which is further emphasised by similar average time required for intestinal food digestion (Walters & Prather, 2013). In addition, pigs has been successfully used to test diagnostic and novel surgical techniques for the benefit of human medicine (Kobayashi, Hishikawa, Teratani, & Lefor, 2012). Minipigs, with Göttingen Minipigs being one of the most popular strain of minipigs, offer all of the above advantages, but in addition their small size and slow growth rate, genetic standardization plus superior health status makes them a more cost-effective and preferred animal model in comparison to domestic farm pigs.

Abbreviations: AAV, adeno-associated virus; BBB, blood brain barrier; Cas9, CRISPR associated protein 9; CMV, cytomegalovirus; CNS, central nervous system; CRISPR, clustered regularly interspaced short palindromic repeats; DAPI, 4′,6-diamidino-2-phenylindole; EGFP, enhanced green fluorescent protein; GENISYST, genomics integrated systems transgenesis; HPRT, hypoxanthine-guanine phosphoribosyltransferase; IHC, immunohistochemistry; ITR, inverted terminal repeat; PBS, phosphate buffered saline; QC, quality control; rAAV, recombinant adeno-associated virus; SE, standard error.

* Corresponding authors.
E-mail addresses: roy.forster@cantab.net (R. Forster), michal@genomebiologics.com (M. Malewicz), Krishnan@med.uni-frankfurt.de (J. Krishnan).

https://doi.org/10.1016/j.vascn.2021.106956
Received 20 July 2020; Received in revised form 3 February 2021; Accepted 8 February 2021
Available online 18 February 2021

In order to derive clinically relevant animal models of human disease, genetic engineering is commonly used to introduce genetic changes required to invoke the disease phenotype. Such genetic alterations involve both gain-of-function and loss-of-function approaches. In the gain-of-function context the typical manipulation involves upregulation of the activity of a desired gene (or genes) in a systemic or in a tissue-specific fashion. There are several common approaches to achieve this in minipigs such as virus-mediated gene transfer and/or CRISPR (clustered regularly interspaced short palindromic repeats) technology (Perleberg, Kind, & Schnieke, 2018; Yum, Yoon, Lee, Lee, & Jang, 2016). Typical generation time for a genetic model using these methods exceeds 2 years. Here we report development of adeno associated virus (AAV) based technology termed Genomics Integrated Systems Transgenesis (GENISYST) for rapid one-step gain-of-function disease modelling in Göttingen Minipigs. Here we have achieved high-level systemic expression of a transgene within weeks of GENISYST administration in multiple disease-relevant tissues of the minipig including liver, heart, brain, kidney, and lungs. In summary our data indicates feasibility of a rapid one-step generation of transgenic minipigs for human disease modelling in drug development.

2. Results

Given the lengthy time frames and substantial resources needed to derive new transgenic minipig strains, we set out to establish a simple and rapid method for gain-of-function trait modelling in these animals. We reasoned that application of viruses might be a promising approach because of their ease of production and the immediate transgene expression potential when delivered orthotopically or systemically. We were particularly inclined to test the usefulness of adeno-associated viruses (AAVs) owing to a long-term transgene expression potential and their high efficiency of cellular transduction (Naso, Tomkowicz, Perry 3rd, & Strohl, 2017). Therefore, we constructed an adeno-associated virus genome-based vector expressing enhanced green fluorescent protein (EGFP) and used it to produce a high-titre recombinant AAV9-EGFP viral particles (Fig. 1A). By virtue of the modular nature of our AAV platform and its capacity to implement complex disease heterogeneity patterns for high-throughput in vivo screens (Krishnan & Ward, 2018), this technology is termed Genomics Integrated Systems Transgenesis (GENISYST). Although administration of recombinant viruses to animals can be performed by a variety of routes (Steitz et al., 2010), we delivered our GENISYST preparations by intra-venous injections (Fig. 1B), as this method had previously showed consistent systemic spread of recombinant AAVs (Lykken, Shyng, Edwards, Rozenberg, & Gray, 2018). To assess the overall quality of our AAV injections and persistence of EGFP expression we performed qPCR analysis to quantify the mean level of mRNA expression in the liver of GENISYST injected animals at 70 days post injection (Fig. 2). This analysis revealed high-level of AAV-derived EGFP mRNA expression as compared to uninjected animals, indicating that our GENISYST preparations efficiently transduced liver tissue and facilitated long-term EGFP expression at 70 days post-transduction (Fig. 2).

Successful disease modelling requires consistent targeting of relevant internal organs such as liver, heart, brain, and others. Thus, we next aimed to determine the tissue distribution of transgenic EGFP protein expressed form our recombinant AAVs. We initially focused our analysis on animals harvested at 14 days post injection to assess the rapidity of GENISYST action. Several vital organs were collected, fixed and processed for immunofluorescent detection with anti-EGFP antibodies. We observed detectable EGFP expression in the liver, heart, kidneys, lungs, brain, small intestine, lymph nodes, and spleen (Figs. 3-8 and Table 1). Particularly high-level expression of EGFP was observed in the liver, whereas heart, kidneys, lung, and the brain showed a more moderate EGFP staining (Table 1). Considering that targeting the central nervous system (CNS) with AAVs remains one of important goals in generation of transgenic animals, our analysis of GENISYST expression in the brain extended into cerebral cortex, thalamus and the cerebellum. While the cerebral cortex and the thalamus showed detectable EGFP immunofluorescence (Figs. 7 and 8) we failed to detect significant EGFP expression in the cerebellum (data not shown).

High expression of AAV-derived transgene in the liver is likely a reflection of a high affinity of AA9 serotype for hepatocytes (Sands, 2011). Most organs exhibited near-uniform expression of EGFP throughout the tissues indicating that almost cell types were successfully transduced by the virus. Strikingly, in the kidney and lung, specialised substructures such as proximal tubules and bronchioles, showed EGFP protein enrichment (Figs. 5 and 6 respectively; Table 1). Localised EGFP expression in the kidney and lung likely reflects virus distribution due to blood flow through these organs, as comparable staining pattern with enrichment in proximal tubules was observed after intravenous injection of a soluble cell-penetrating fluorochrome (Sandoval, Kennedy, Low, & Molitoris, 2004). Thus, GENISYST achieved efficient targeting of vital organs already at 14 days after administration.

Encouraged by our data with fluorescent anti-EGFP protein detection in multiple tissues at 14 days post-injection (Figs. 3-8) we next aimed to corroborate our findings in animals harvested 70 days after GENISYST administration. We focused on the heart and the kidney due to the high unmet need for disease models involving those organs. As previously described, we detected strong mRNA EGFP expression levels at 70 days post injection in the liver (Fig. 2). We next stained deparaffinised tissue sections for EGFP, with haematoxylin/eosin counterstaining to visualise tissue ultrastructure (Fig. 9). This approach demonstrated prominent EGFP staining throughout the cardiac epicardium (top part of the image in Fig. 9B) but also in the myocardium (bottom part of the image in

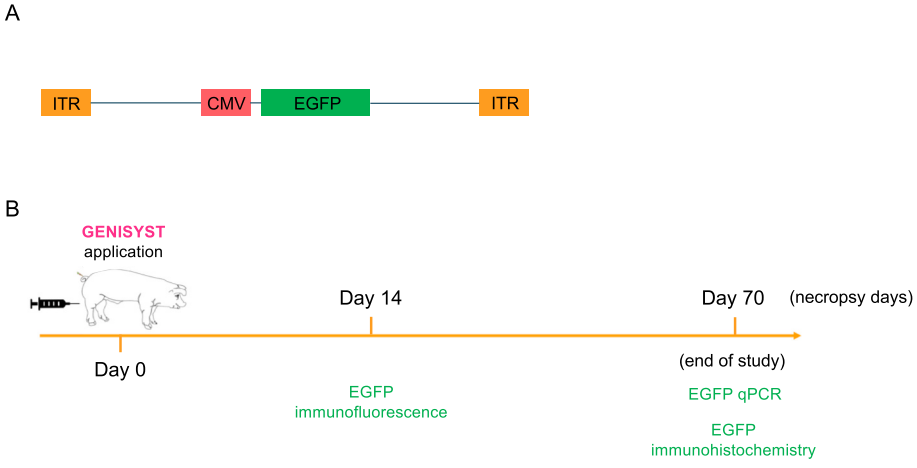

Fig. 1. Schematic drawing of the GENISYST DNA construct and the experimental design. A) Schematic representation of the recombinant AAV (GENISYST) DNA genome. (ITR) – inverted terminal repeat sequence, (CMV) – cytomegalovirus promoter, (EGFP) – EGFP encoding cDNA sequence. B) Göttingen Minipigs were injected with GENISYST at Day 0 and harvested for necropsy at indicated time points. Green text boxes indicate EGFP detection assays performed at indicated time points. (For interpretation of the references to colour in this figure legend, the reader is referred to the web version of this article.)

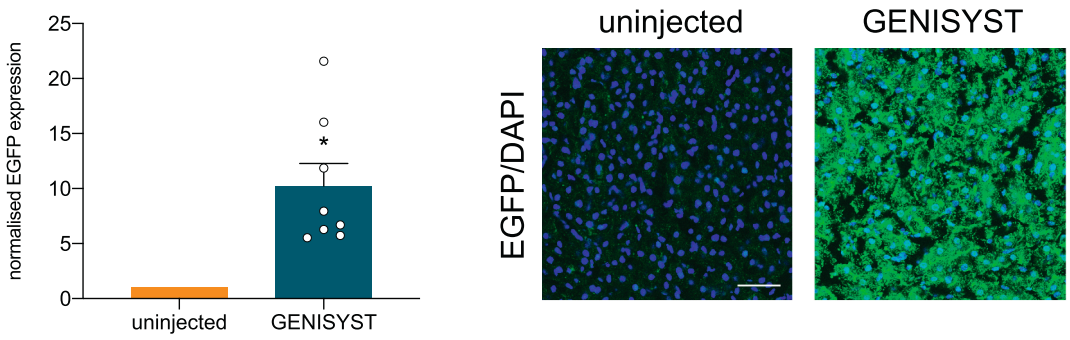

Fig. 2. Analysis of EGFP expression by qPCR in the liver. The graph presents mean expression levels of EGFP mRNA normalized to HPRT housekeeping gene as determined by qPCR (mean value for uninjected animals was set to 1). Representative images for EGFP signal in frozen sections are shown on the right. White scale bar corresponds to 50 μm in length. Uninjected animals ($n = 2$) serve as a negative control for background qPCR amplification. GENISYST animals ($n = 8$) were injected with AAVs. White circles represent EGFP expression levels in individual animals. Error bars represent SE of the mean. Animals were harvested at day 70 after injection. Asterisk (*) indicates statistical significance with the $p < 0.05$ by 2-tailed unpaired *t*-test against uninjected group.

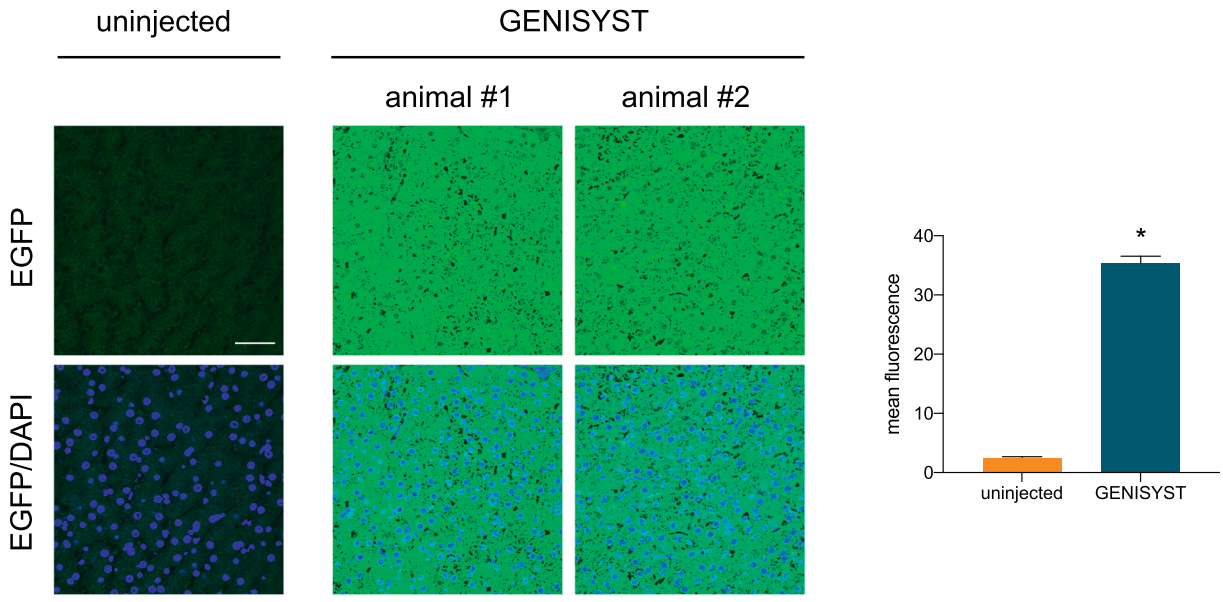

Fig. 3. Analysis of EGFP expression by immunofluorescence in the liver. Uninjected indicates negative control animals; GENISYST denotes animals that received AAV injection. DAPI indicates the position of nuclei. Representative images are shown. Bar graphs represent the quantification of the fluorescent EGFP signal. Error bars represent SE of the mean. Animals were harvested 14 days after injection (n = 2 for both uninjected and GENISYST group). Asterisk (*) indicates statistical significance with the $p < 0.05$ by 2-tailed unpaired t-test against uninjected group. Scale bar corresponds to 50 μm in length.

Fig. 9B). In the kidney, in agreement with previously obtained data (Fig. 5), an enrichment of EGFP signal was observed in proximal tubules and in the glomeruli (Fig. 9A). In conclusion our experiments with GENISYST EGFP-expressing rAAVs resulted in a systemic delivery of EGFP protein to most tissues achieving both early and persistent expression - therefore demonstrating the potential utility of this approach for human gain- or loss-of-function disease modelling in minipigs.

3. Discussion

Over the years several approaches to the establishment of genetically modified minipigs had been undertaken. For example, CRISPR technology (clustered regularly interspaced short palindromic repeats) was recently applied to generate a type 2 diabetic minipig model (Zou et al., 2019). In that report, CRISPR was used to insert a transgene encoding human Islet amyloid polypeptide (IAPP, amylin) into a minipig chromosome. The procedure involved in vitro genetic modification of porcine foetal fibroblasts with the help of CRISPR associated protein 9 (Cas9) to induce chromosome cleavage for targeted IAPP transgene integration. Thereafter, selected modified fibroblast clones served as a nucleus donor for somatic nuclear transfer procedure to derive genetically altered minipig line expressing the IAPP protein. In another study, *proprotein convertase subtilisin/kexin type 9* (*PCSK-9*) gene gain-of-function founders were generated in minipig by the use of engineered *Sleeping Beauty* transposons resulting in a phenotype resembling human congenital syndrome of familial hypercholesterolemia (Yuan et al., 2018). Herein, the derivation of *PCSK-9* gain-of-function minipigs also required an initial in vitro fibroblast transfection with transposons followed by somatic nuclear transfer to establish founder lines. Other approaches to genetically altered minipig production involved the use of lentiviruses to infect porcine embryos, which resulted in a persistent overexpression of a gene encoding human huntingtin (HTT) to create a minipig model of Huntington's Disease (Ardan et al., 2019; Baxa et al., 2013). All of the above-mentioned approaches, while successful in generation of useful minipig disease models, required a long production time. In contrast, one of the advantages of AAVs is the immediate cell transduction and stable long-term expression of the encoded transgene

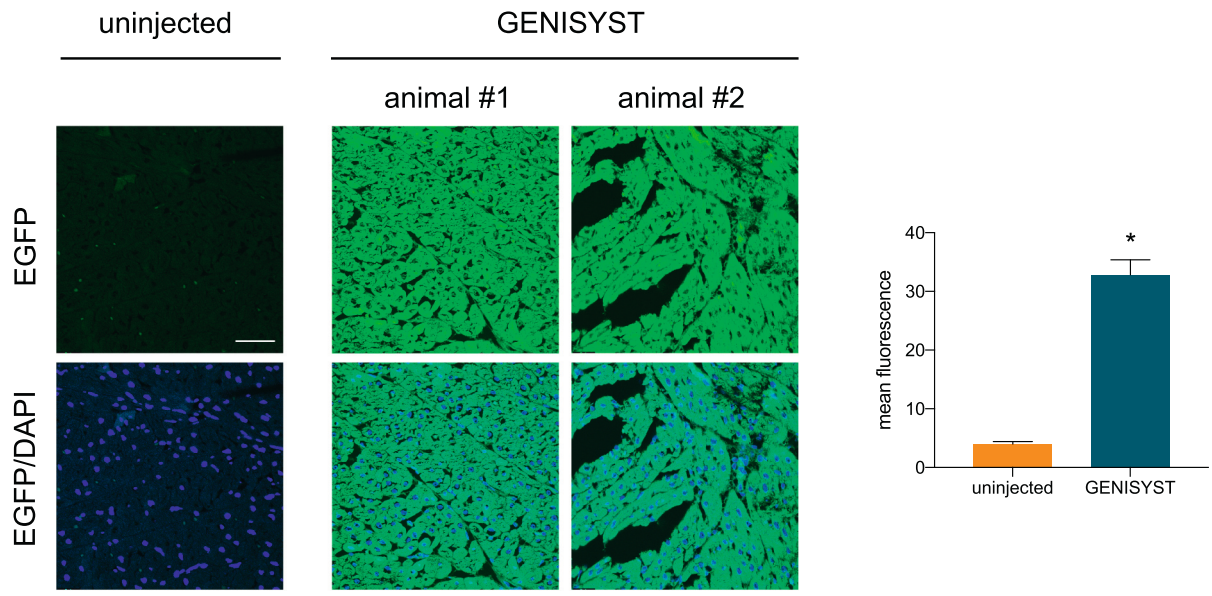

Fig. 4. Analysis of EGFP expression by immunofluorescence in the heart. Uninjected indicates negative control animals; GENISYST denotes animals that received AAV injection. DAPI indicates the position of nuclei. Representative images are shown. Bar graphs represent the quantification of the fluorescent EGFP signal. Error bars represent SE of the mean. Animals were harvested 14 days after injection (n = 2 for both uninjected and GENISYST group). Asterisk (*) indicates statistical significance with the $p < 0.05$ by 2-tailed unpaired t-test against uninjected group. White scale bar corresponds to 50 μm in length.

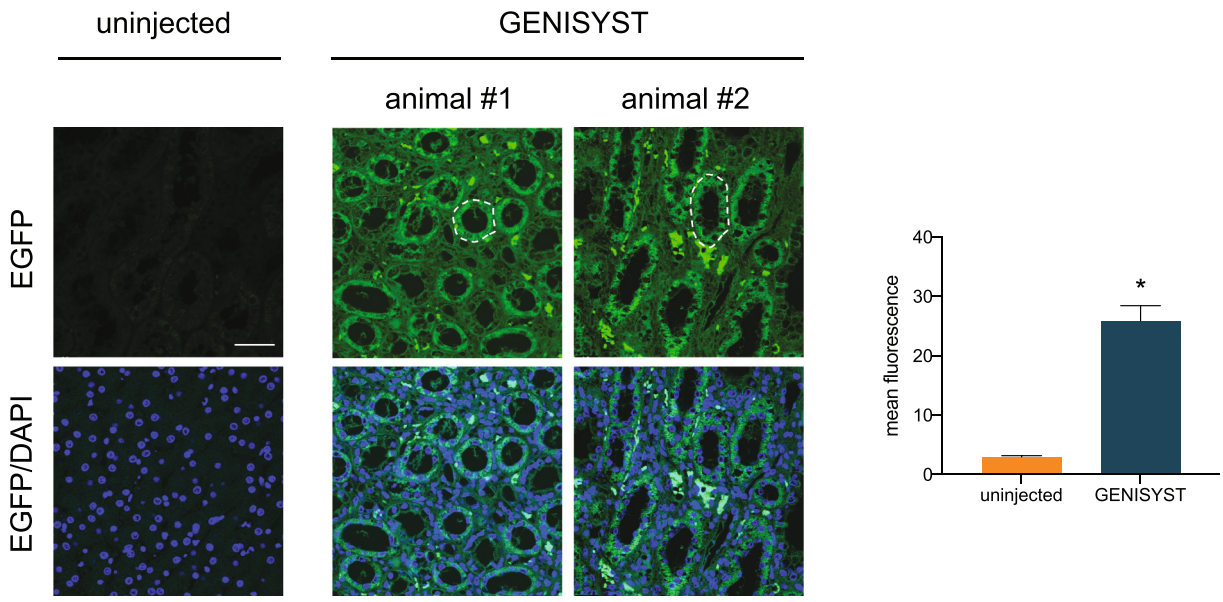

Fig. 5. Analysis of EGFP expression by immunofluorescence in the kidney. Uninjected indicates negative control animals; GENISYST denotes animals that received AAV injection. DAPI indicates the position of nuclei. White dashed lines mark the position of a proximal tubules. Representative images are shown. Bar graphs represent the quantification of the fluorescent EGFP signal. Error bars represent SE of the mean. Animals were harvested 14 days after injection (n = 2 for both uninjected and GENISYST group). Asterisk (*) indicates statistical significance with the $p < 0.05$ by 2-tailed unpaired t-test against uninjected group. Scale bar corresponds to 50 μm in length.

(Wang, Tai, & Gao, 2019). These features are clearly exemplified by the results we have achieved with our GENISYST approach. We would like to highlight that our method is not meant to replace approaches that utilise stable minipig genome DNA sequence change resulting in subsequent derivation of animal strains with heritable characteristics. GENISYST represents an ad hoc method of rapid genetic minipig modification that will complement the existing methodologies.

The knowledge of AAV biology is steadily increasing allowing for continued progress in AAVs engineering for the purpose of disease modelling and gene therapy. For example, several AAV serotypes utilised in biotechnology offer a diversity in capsid surface topology that is responsible for different antigenicity, tissue tropism and target receptor affinity (Steines et al., 2016). Furthermore, novel AAV types with clinically useful profiles are being made by reengineering the capsid surface of AAVs. A number of chimeric AAV libraries were generated by laboratories around the world and some achieved significant success in specific therapeutic purposes (Fakhiri et al., 2019). For example, gene therapy specifically targeting the muscle using a chimeric AAV had entered the clinical trial (Colella, Ronzitti, & Mingozzi, 2018). Based on all of the progress in the AAV engineering, further development of the

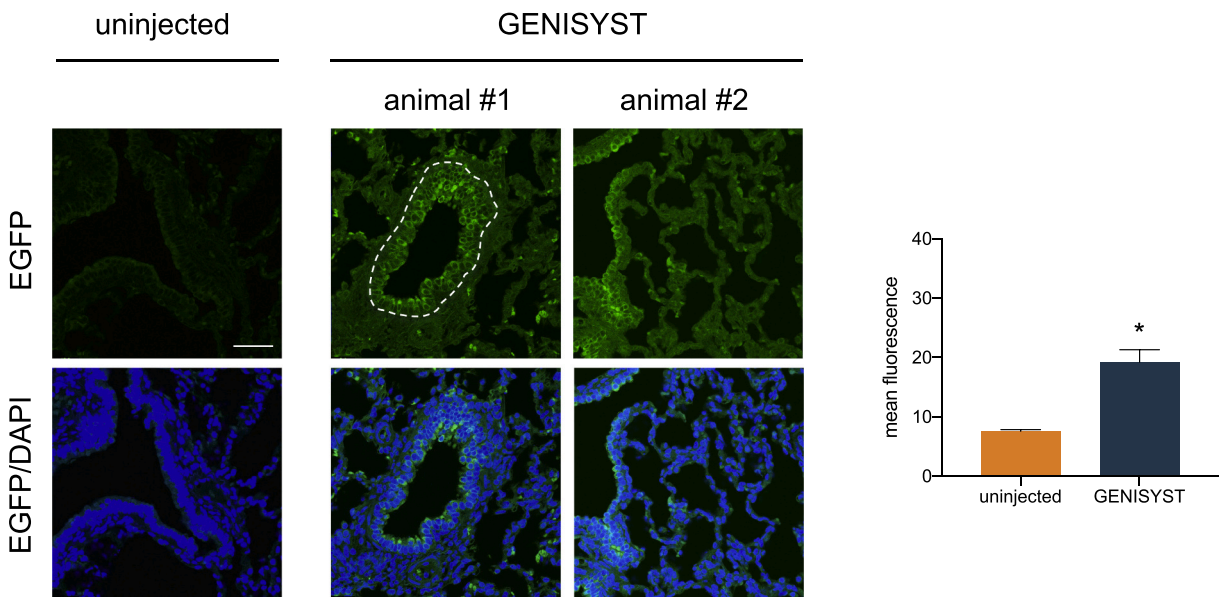

Fig. 6. Analysis of EGFP expression by immunofluorescence in the lung. (Uninjected) indicates negative control animals; (GENISYST) denotes animals that received AAV injection. DAPI indicates the position of nuclei. White dashed line marks the position of a bronchiole. Representative images are shown. Bar graphs represent the quantification of the fluorescent EGFP signal. Error bars represent SE of the mean. Animals were harvested 14 days after injection (n = 2 for both uninjected and GENISYST group). Asterisk (*) indicates statistical significance with the $p < 0.05$ by 2-tailed unpaired t-test against uninjected group. Scale bar corresponds to 50 μm in length.

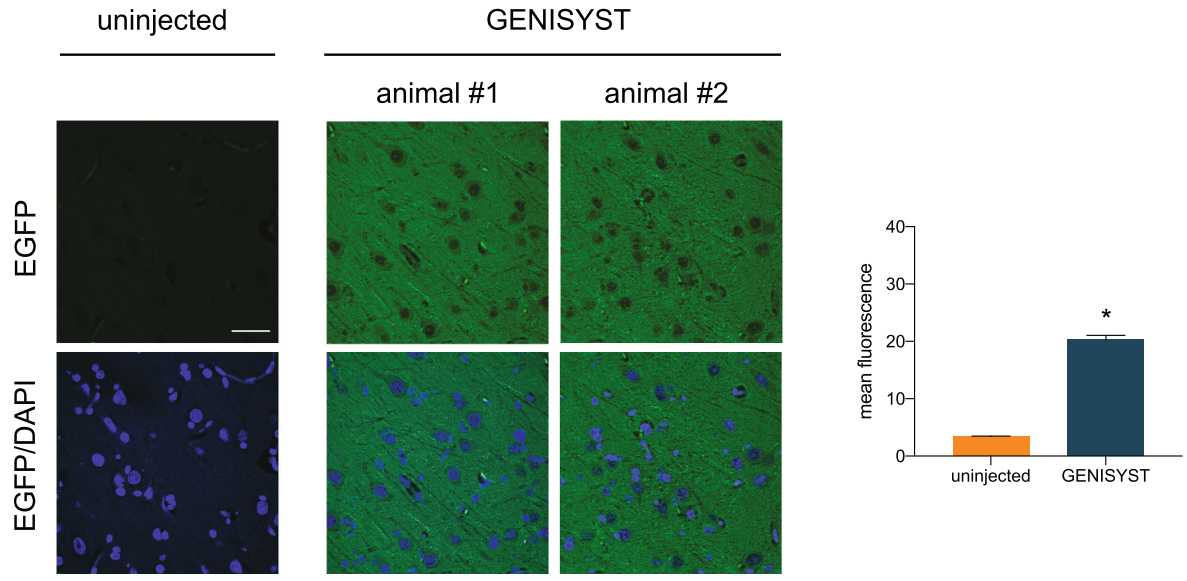

Fig. 7. Analysis of EGFP expression by immunofluorescence in the cerebral cortex of the brain. Uninjected indicates negative control animals; GENISYST denotes animals that received AAV injection. DAPI indicates the position of nuclei. Representative images are shown. Bar graphs represent the quantification of the fluorescent EGFP signal. Error bars represent SE of the mean. Animals were harvested 14 days after injection (n = 2 for both uninjected and GENISYST group). Asterisk (*) indicates statistical significance with the $p < 0.05$ by 2-tailed unpaired t-test against uninjected group. Scale bar corresponds to 50 μm in length.

GENISYST technology will aim to achieve tissue-restricted AAV tropism allowing for more precise organ-specific disease modelling in animals.

Another strategy to achieve localised AAV action, in order to lower the probability of undesired remote effects, is to deliver the AAVs directly to the target tissue (White et al., 2004). Indeed, a recent study substantially improved cardiac function in a chronic heart failure (HF) model by overexpression of constitutively active inhibitor-1 (I-1c) using a novel cardiotropic vector generated by capsid reengineering of adeno-associated virus. This had been achieved by intra-cardiac injection of a cardiotropic vector for heart-specific gene transfer in a clinically relevant animal model (Ishikawa et al., 2014). Apart from AAVs also lentiviruses had been tested in localised administration regimes. For example, direct gene transfer to the central nervous system (CNS) had been described in minipigs using intra cranial stereotaxic frame-assisted administration (Norgaard Glud et al., 2010). Because of these successful examples, it would also be of interest to test the applicability of GENISYST when administered directly to the target tissue under study.

Another feature of systemic AAV delivery is its ability to target the central nervous system (CNS). CNS is guarded by the blood-brain barrier (BBB), which serves to protect the spinal cord and the brain homeostasis

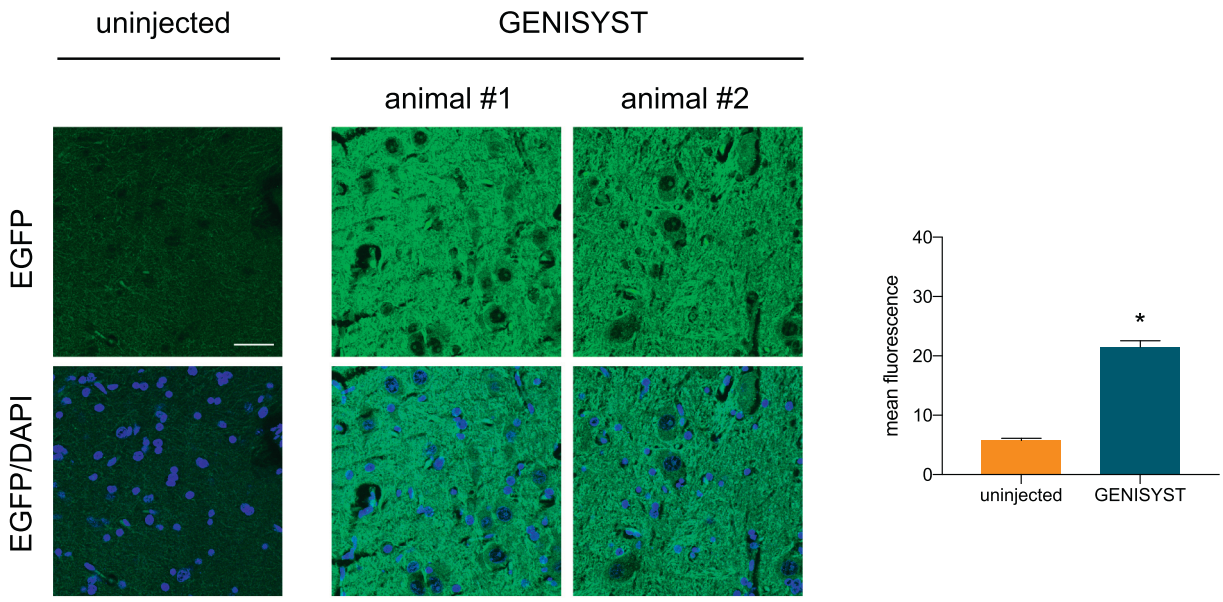

Fig. 8. Analysis of EGFP expression by immunofluorescence in the thalamus region of the brain. Uninjected indicates negative control animals; GENISYST denotes animals that received AAV injection. DAPI indicates the position of nuclei. Representative images are shown. Bar graphs represent the quantification of the fluorescent EGFP signal. Error bars represent SE of the mean. Animals were harvested 14 days after injection (n = 2 for both uninjected and GENISYST group). Asterisk (*) indicates statistical significance with the $p < 0.05$ by 2-tailed unpaired t-test against uninjected group. Scale bar corresponds to 50 μm in length.

Table 1
List of tissues showing EGFP expression by immunofluorescence in the minipig.

Tissue	EGFP expression	Comments
Liver	++++	
Heart	+++	detected in epicardium and myocardium
Kidney	+++	enriched in proximal tubules and glomeruli
Lung	++	enriched in bronchioles
Brain (cerebral cortex)	++	
Brain (thalamus)	++	
Spleen	++	
Small intestine	+	
Lymph node	+	

(++++,+++, ++, +) indicate graded EGFP signal as compared to the uninjected animal control according to the criteria described in Materials and Methods.

by limiting the spectrum of molecules able to penetrate across the BBB. Although AAV as such is able to pass the BBB, there exist a great variability between AAV serotypes in terms of their relative BBB passing efficiency (Zhang et al., 2011). In addition, depending on the age of the animal the propensity to preferentially infect neurones over glial cells was previously observed (Foust et al., 2009). Strong interest in targeting the CNS yielded new artificial AAV variants that show even stronger CNS-targeting ability than the naturally occurring AAV serotypes such as the AAV9 (Deverman et al., 2016). In agreement with our data, recent work demonstrated that AAVs can be used to deliver therapeutically relevant transgenes to the minipig CNS (Evers et al., 2018). Although collectively these reports suggest that successful targeting of CNS with systemically delivered AAVs is possible, care must be taken to analyse the performance of each rAAV variant (and the application route) in terms of location in different brain regions, as substantial variability still exist here. For example, GENISYST appears to efficiently target cerebral cortex and thalamus making it suitable for modelling diseases that affect these brain regions.

It is worth mentioning that for any further GENISYST applications the QC criteria defining animal selection for further studies will be an important consideration. Such criteria should include confirmation of consistency for transgene expression and of the phenotype establishment as well as definition of essential downstream functional assays. It is anticipated that many of QC criteria will be specific to modelled disease. Progression of disease should also be assessed by harvesting animals at different timepoints to define the best timeframe for further studies.

Although a multitude of approaches had been developed to model gain-of-function traits in minipigs, most of them incur both long

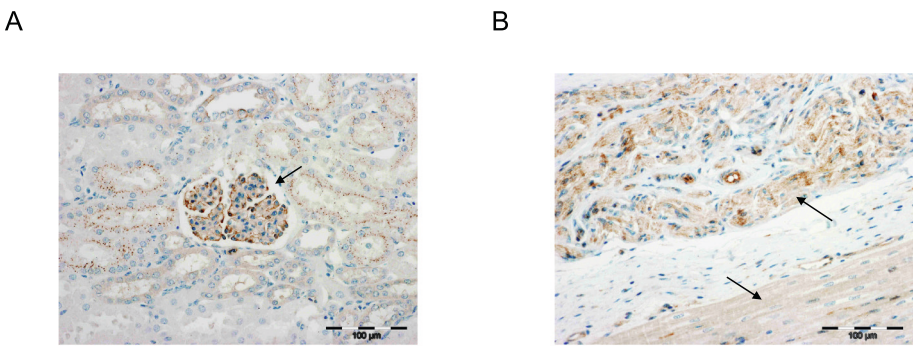

Fig. 9. Analysis of EGFP expression by immunohistochemistry in the kidney and the heart. A) Anti-EGFP immunohistochemistry stain of a kidney section from GENISYST injected animal. Black arrow depicts the position of a glomeruli. B) Anti-EGFP immunohistochemistry stain of a heart section from GENISYST injected animal. Top black arrow depicts the location of a cardiac epicardium, bottom arrow points to the myocardium. Dark brown colour indicates EGFP signal. Representative images are shown. Animals were harvested 70 days after injection. Scale bar corresponds to 100 μm in length. (For interpretation of the references to colour in this figure legend, the reader is referred to the web version of this article.)

generation times and a significant cost (Uchida et al., 2001). In stark contrast to those methods, GENISYST technology described here is fast, cost-effective and efficient. In summary, our data demonstrated a feasibility of using recombinant AAVs for rapid generation of transgenic Göttingen Minipigs with the aim of human disease modelling for drug discovery and development. Our approach offers significant benefits of a short time frame needed for model generation and a reduction in animals used for the experiments. Thus, our platform allows for significant cost savings over traditional methods.

4. Materials and methods

4.1. Animal treatment

The study was performed in 12 male Göttingen Minipigs (Ellegaard Göttingen Minipigs A/S, Denmark); obtained by the age of 8 weeks. In brief, animals were housed in a room provided with filtered air at a temperature of 24 °C, 15 air changes per hour and a cycle of 12 h light and 12 h darkness. Minipigs were fed a minipig diet (SMP (E) SQC) from (SDS, UK) twice daily. For environmental enrichment, animals were offered ice cubes, either plain or containing A-38 (a commercially available acidified milk product) or pieces of the minipig diet. Animals had an ad libitum access to drinking water. This project has been approved by the Danish Authorities under reference number 2015-15-0201-00713. All animal experiments were carried out in accordance with EU Directive 2010/63/EU for animal experiments.

4.2. AAV generation

GENISYST DNA construct is based on pAAV-BASIC-EGFP plasmid, in which EGFP marker gene is expressed from a ubiquitously active CMV promoter (Fig. 1A). AAV9 viruses were manufactured by Vector Biolabs (Malvern, USA) by co-transfection of pAAV-BASIC-EGFP with AdHelper vector and AAV Rep/Cap vector into a packaging cell line followed by purification of the virus-containing supernatant on caesium chloride gradient. Concentrated virus stocks ($\geq 10^{13}$ GC/ml) were kept at minus 80 °C prior to use.

4.3. AAV application

For the AAV application, the animals were sedated with a combination of ketamine (6.25 mg/kg body weight; Veterinaria, AG Switzerland) and midazolam (1.25 mg/kg bodyweight of 5 mg/mL; Veterinaria, AG Switzerland), given as intramuscular injection. In total 10 animals were injected with AAVs at final concentration of 8.0×10^{12} GC/kg. Two animals were harvested at 14 days after AAV injection and eight animals were harvested 70 days after AAV application (Fig. 1B). Two additional naïve animals were used as uninjected negative controls.

4.4. qPCRs

At sacrifice, a sample of the liver lobe was snap frozen in liquid nitrogen. Expression of the EGFP gene was evaluated by RT-PCR according to the following protocol:

Small liver tissue biopsies were homogenised (MP Homogeniser FastPrep) in RLT buffer and total RNA was extracted with RNAeasy kit (Qiagen). Total RNA was converted to cDNA with the use of oligo-dT-primed EcoDry cDNA synthesis kit (TaKaRa). QPCR reactions were run with SybrGreen-containing premix (Applied Biosystems) and run on StepOnePlus qPCR machine (Applied Biosystems). Raw data was exported Excel (Microsoft) and gene expression changes were calculated by a delta/delta Ct method. Expression of EGFP was normalized to housekeeping gene levels (HPRT). Statistical analysis was performed with an unpaired 2-tailed *t*-test in Prism (GraphPad software). Primer sequences used for qPCR: HPRT (forward primer: ATTCTTTGCTGACCTGCTG; reverse primer: TCTTTGGATTATGCTGCTTGAC) and EGFP (forward primer: CTACCCCGACCACATGAAGC; reverse primer: AAGTCGATGCCCTTCAGCTC).

4.5. Organ harvest and processing

After the animals were sacrificed for necropsy, all tissues were initially fixed in phosphate buffered neutral 4% formaldehyde with the exception of the eyes and testes (Modified Davidson's fixative). The fixative for long term preservation was phosphate buffered neutral 4% formaldehyde for all tissues. The lungs were infused with fixative at necropsy. Samples for histopathological evaluation from all animals were trimmed and representative specimens were progressed for histological processing. The specimens were embedded in paraffin.

4.6. Immunofluorescent EGFP staining and immunohistochemical EGFP staining

Frozen liver sections (only Fig. 2) were cut at 10 μm after embedding the fresh tissue in OCT medium. Sections were thawed at room temperature, fixed in cold 4% paraformaldehyde and then blocked for 30 min at 4 °C in blocking buffer (Phosphate Buffer Saline containing 1% normal goat serum and 0.3% Triton-X100) followed by incubation overnight in blocking buffer containing anti-EGFP primary antibodies (1:100 dilution; cat. A-11120; ThermoFisherScientific). Thereafter the slides were washed extensively with PBS and incubated in room temperature in blocking buffer containing AlexaFluor488-labelled secondary antibodies (1:500 dilution; ThermoFisherScientific) and DAPI counterstain to visualise the nuclei. After additional washes in PBS slides were mounted in Prolonged Gold antifade (ThermoFisherScientific), allowed to solidify and then imaged on a Leica TCS SP8 confocal microscope.

Paraffin embedded organs were sectioned at 6 μm on a microtome, deparaffinised and following antigen retrieval (boiling for 15 min in 10 mM sodium citrate, 0.05% Tween 20, pH 6.0) processed for immunofluorescence with anti-EGFP antibodies. Briefly, slides were blocked for 30 min at 4 °C in blocking buffer (Phosphate Buffer Saline containing 1% normal goat serum and 0.3% Triton-X100) and then incubated overnight in blocking buffer containing anti-EGFP primary antibodies (1:100 dilution; cat. A-11120; ThermoFisherScientific). Thereafter the slides were washed extensively with PBS and incubated in room temperature in blocking buffer containing AlexaFluor488-labelled secondary antibodies (1:500 dilution; ThermoFisherScientific) and DAPI counterstain to visualise the nuclei. After additional washes in PBS slides were mounted in Prolonged Gold antifade (ThermoFisherScientific), allowed to solidify and then imaged on a Leica TCS SP8 confocal microscope.

Images were carefully sampled to be representative of the respective tissue with similar tissue density and tissue region chosen for comparison. For each animal/tissue five representative sections were used for quantification. EGFP immunofluorescence signal was quantified with ImageJ software (NIH, USA). The statistical significance by 2-tailed unpaired *t*-test was assessed in Prism (GraphPad software). For grading tissue EGFP signal intensity (Table 1) mean fluorescence intensity signal from uninjected animals (background staining) was subtracted from signal measured in GENISYST injected animals to obtain normalized mean fluorescent intensity. EGFP signal was graded "++++" for normalized mean fluorescent intensity values above 30, "+++" for values between 30 and 20, "++" for values below 20 and above 10 and "+" for values below 10.

For immunocytochemistry (IHC) staining (Fig. 9) paraffin embedded organs were sectioned at 5 μm on a microtome, deparaffinised, and then following antigen retrieval step processed for EGFP staining signal with rabbit anti-EGFP antibodies (ab6556; Abcam) and after counter staining with haematoxylin and eosin visualised with the help of Ventana Discovery instrument.

Declaration of interests

The authors declare that they have no known competing financial interests or personal relationships that could have appeared to influence the work reported in this paper.

CRediT authorship contribution statement

Joachim Maxeiner: Investigation. Rahul Sharma: Software, Resources. Carolin Amrhein: Investigation. Frederic Gervais: Data curation, Supervision. Maria Duda: Writing - review & editing, Project administration. Jonathan Ward: Conceptualization, Project administration, Funding acquisition. Lars Friis Mikkelsen: Conceptualization, Writing - review & editing, Project administration, Funding acquisition. Roy ForsterConceptualization, Writing - review & editing. Michal Malewicz: Investigation, Data curation, Writing - original draft. Jaya Krishnan: Conceptualization, Supervision, Writing - review & editing, Project administration, Funding acquisition.

Funding sources

This work was supported by grants from the European Union Horizon 2020/EIC (822455), Ellegaard Göttingen Minipigs Research Foundation and in-kind contributions from Citoxlab.

Acknowledgments

We are grateful to all members of Genome Biologics and the Institute for Cardiovascular Regeneration, and in particular Ting Yuan for scientific and technical advice and support. We would also like to thank Marianne Kronborg Bracken and Charles River Laboratories Copenhagen A/S for valuable discussions and for helping with sample handling.

References

Ardan, T., Baxa, M., Levinska, B., Sedlackova, M., Nguyen, T. D., Klima, J., … Ellederova, Z. (2019). Transgenic minipig model of Huntington's disease exhibiting gradually progressing neurodegeneration. *Disease Models & Mechanisms, 13*(2). https://doi.org/10.1242/dmm.041319.

Baxa, M., Hruska-Plochan, M., Juhas, S., Vodicka, P., Pavlok, A., Juhasova, J., … Motlik, J. (2013). A transgenic minipig model of Huntington's disease. *Journal of Huntington's Disease, 2*(1), 47–68. https://doi.org/10.3233/JHD-130001.

Colella, P., Ronzitti, G., & Mingozzi, F. (2018). Emerging issues in AAV-mediated in vivo gene therapy. *Molecular Therapy — Methods & Clinical Development, 8*, 87–104. https://doi.org/10.1016/j.omtm.2017.11.007.

Deverman, B. E., Pravdo, P. L., Simpson, B. P., Kumar, S. R., Chan, K. Y., Banerjee, A., … Gradinaru, V. (2016). Cre-dependent selection yields AAV variants for widespread gene transfer to the adult brain. *Nature Biotechnology, 34*(2), 204–209. https://doi.org/10.1038/nbt.3440.

Evers, M. M., Miniarikova, J., Juhas, S., Valles, A., Bohuslavova, B., Juhasova, J., … Konstantinova, P. (2018). AAV5-miHTT gene therapy demonstrates broad distribution and strong human mutant huntingtin lowering in a Huntington's disease minipig model. *Molecular Therapy, 26*(9), 2163–2177. https://doi.org/10.1016/j.ymthe.2018.06.021.

Fakhiri, J., Schneider, M. A., Puschhof, J., Stanifer, M., Schildgen, V., Holderbach, S., … Grimm, D. (2019). Novel chimeric gene therapy vectors based on adeno-associated virus and four different mammalian bocaviruses. *Molecular Therapy — Methods & Clinical Development, 12*, 202–222. https://doi.org/10.1016/j.omtm.2019.01.003.

Forster, R., Bode, G., Ellegaard, L., van der Laan, J. W., & Steering Group of the, R. P. (2010). The RETHINK project–minipigs as models for the toxicity testing of new medicines and chemicals: An impact assessment. *Journal of Pharmacological and Toxicological Methods, 62*(3), 158–159. https://doi.org/10.1016/j.vascn.2010.05.003.

Foust, K. D., Nurre, E., Montgomery, C. L., Hernandez, A., Chan, C. M., & Kaspar, B. K. (2009). Intravascular AAV9 preferentially targets neonatal neurons and adult astrocytes. *Nature Biotechnology, 27*(1), 59–65. https://doi.org/10.1038/nbt.1515.

Ishikawa, K., Fish, K. M., Tilemann, L., Rapti, K., Aguero, J., Santos-Gallego, C. G., … Hajjar, R. J. (2014). Cardiac I-1c overexpression with reengineered AAV improves cardiac function in swine ischemic heart failure. *Molecular Therapy, 22*(12), 2038–2045. https://doi.org/10.1038/mt.2014.127.

Kobayashi, E., Hishikawa, S., Teratani, T., & Lefor, A. T. (2012). The pig as a model for translational research: Overview of porcine animal models at Jichi Medical University. *Transplantation Research, 1*(1), 8. https://doi.org/10.1186/2047-1440-1-8.

Krishnan, J., & Ward, J. (2018). Tissue selective transgene expression. *United States Patent and Trademark Office. USA, Genome Biologics.*

Luo, Y., Lin, L., Bolund, L., Jensen, T. G., & Sorensen, C. B. (2012). Genetically modified pigs for biomedical research. *Journal of Inherited Metabolic Disease, 35*(4), 695–713. https://doi.org/10.1007/s10545-012-9475-0.

Lykken, E. A., Shyng, C., Edwards, R. J., Rozenberg, A., & Gray, S. J. (2018). Recent progress and considerations for AAV gene therapies targeting the central nervous system. *Journal of Neurodevelopmental Disorders, 10*(1), 16. https://doi.org/10.1186/s11689-018-9234-0.

Naso, M. F., Tomkowicz, B., Perry, W. L., 3rd, & Strohl, W. R. (2017). Adeno-associated virus (AAV) as a vector for gene therapy. *BioDrugs, 31*(4), 317–334. https://doi.org/10.1007/s40259-017-0234-5.

Norgaard Glud, A., Hedegaard, C., Nielsen, M. S., Sorensen, J. C., Bendixen, C., Jensen, P. H., … Bjarkam, C. R. (2010). Direct gene transfer in the Gottingen minipig CNS using stereotaxic lentiviral microinjections. *Acta Neurobiologiae Experimentalis (Wars), 70*(3), 308–315. Retrieved from https://www.ncbi.nlm.nih.gov/pubmed/20871651.

Perleberg, C., Kind, A., & Schnieke, A. (2018). Genetically engineered pigs as models for human disease. *Disease Models & Mechanisms, 11*(1). https://doi.org/10.1242/dmm.030783.

Rogers, C. S., Stoltz, D. A., Meyerholz, D. K., Ostedgaard, L. S., Rokhlina, T., Taft, P. J., … Welsh, M. J. (2008). Disruption of the CFTR gene produces a model of cystic fibrosis in newborn pigs. *Science, 321*(5897), 1837–1841. https://doi.org/10.1126/science.1163600.

Sandoval, R. M., Kennedy, M. D., Low, P. S., & Molitoris, B. A. (2004). Uptake and trafficking of fluorescent conjugates of folic acid in intact kidney determined using intravital two-photon microscopy. *American Journal of Physiology. Cell Physiology, 287*(2), C517–C526. https://doi.org/10.1152/ajpcell.00006.2004.

Sands, M. S. (2011). AAV-mediated liver-directed gene therapy. *Methods in Molecular Biology, 807*, 141–157. https://doi.org/10.1007/978-1-61779-370-7_6.

Steines, B., Dickey, D. D., Bergen, J., Excoffon, K. J., Weinstein, J. R., Li, X., … Zabner, J. (2016). CFTR gene transfer with AAV improves early cystic fibrosis pig phenotypes. *JCI Insight, 1*(14), Article e88728. https://doi.org/10.1172/jci.insight.88728.

Steitz, J., Wagner, R. A., Bristol, T., Gao, W., Donis, R. O., & Gambotto, A. (2010). Assessment of route of administration and dose escalation for an adenovirus-based influenza A virus (H5N1) vaccine in chickens. *Clinical and Vaccine Immunology, 17*(9), 1467–1472. https://doi.org/10.1128/CVI.00180-10.

Uchida, M., Shimatsu, Y., Onoe, K., Matsuyama, N., Niki, R., Ikeda, J. E., & Imai, H. (2001). Production of transgenic miniature pigs by pronuclear microinjection. *Transgenic Research, 10*(6), 577–582. https://doi.org/10.1023/a:1013059917280.

Walters, E. M., & Prather, R. S. (2013). Advancing swine models for human health and diseases. *Missouri Medicine, 110*(3), 212–215. Retrieved from https://www.ncbi.nlm.nih.gov/pubmed/23829105.

Wang, D., Tai, P. W. L., & Gao, G. (2019). Adeno-associated virus vector as a platform for gene therapy delivery. *Nature Reviews. Drug Discovery, 18*(5), 358–378. https://doi.org/10.1038/s41573-019-0012-9.

White, S. J., Nicklin, S. A., Buning, H., Brosnan, M. J., Leike, K., Papadakis, E. D., … Baker, A. H. (2004). Targeted gene delivery to vascular tissue in vivo by tropism-modified adeno-associated virus vectors. *Circulation, 109*(4), 513–519. https://doi.org/10.1161/01.CIR.0000109697.68832.5D.

Yuan, F., Guo, L., Park, K. H., Woollard, J. R., Taek-Geun, K., Jiang, K., … Carlson, D. F. (2018). Ossabaw pigs with a PCSK9 gain-of-function mutation develop accelerated coronary atherosclerotic lesions: A novel model for preclinical studies. *Journal of the American Heart Association, 7*(6). https://doi.org/10.1161/JAHA.117.006207.

Yum, S. Y., Yoon, K. Y., Lee, C. I., Lee, B. C., & Jang, G. (2016). Transgenesis for pig models. *Journal of Veterinary Science, 17*(3), 261–268. https://doi.org/10.4142/jvs.2016.17.3.261.

Zhang, H., Yang, B., Mu, X., Ahmed, S. S., Su, Q., He, R., … Gao, G. (2011). Several rAAV vectors efficiently cross the blood-brain barrier and transduce neurons and astrocytes in the neonatal mouse central nervous system. *Molecular Therapy, 19*(8), 1440–1448. https://doi.org/10.1038/mt.2011.98.

Zou, X., Ouyang, H., Yu, T., Chen, X., Pang, D., Tang, X., & Chen, C. (2019). Preparation of a new type 2 diabetic miniature pig model via the CRISPR/Cas9 system. *Cell Death & Disease, 10*(11), 823. https://doi.org/10.1038/s41419-019-2056-5.